Dual-purpose isocyanides produced by *Aspergillus fumigatus* contribute to cellular copper sufficiency and exhibit antimicrobial activity

Nicholas Raffa[a], Tae Hyung Won[b], Andrew Sukowaty[a], Kathleen Candor[c], Chengsen Cui[d], Saayak Halder[d], Mingji Dai[d], Julio A. Landero-Figueroa[e], Frank C. Schroeder[b], and Nancy P. Keller[a,f,1]

[a]Department of Medical Microbiology and Immunology, University of Wisconsin–Madison, Madison, WI 53706; [b]Boyce Thompson Institute and Department of Chemistry and Chemical Biology, Cornell University, Ithaca, NY 14853; [c]Agilent Metallomics Center of the Americas, Department of Chemistry, University of Cincinnati College of Arts and Science, Cincinnati, OH 45221; [d]Department of Chemistry and Center for Cancer Research, Purdue University, West Lafayette, IN 47906; [e]Department of Pharmacology and System Biology, University of Cincinnati College of Medicine, Cincinnati, OH 45267; and [f]Department of Bacteriology, University of Wisconsin–Madison, Madison, WI 53706

Edited by Joan Wennstrom Bennett, Rutgers, The State University of New Jersey, New Brunswick, NJ, and approved January 11, 2021 (received for review July 24, 2020)

The maintenance of sufficient but nontoxic pools of metal micronutrients is accomplished through diverse homeostasis mechanisms in fungi. Siderophores play a well established role for iron homeostasis; however, no copper-binding analogs have been found in fungi. Here we demonstrate that, in *Aspergillus fumigatus*, xanthocillin and other isocyanides derived from the *xan* biosynthetic gene cluster (BGC) bind copper, impact cellular copper content, and have significant metal-dependent antimicrobial properties. *xan* BGC-derived isocyanides are secreted and bind copper as visualized by a chrome azurol S (CAS) assay, and inductively coupled plasma mass spectrometry analysis of *A. fumigatus* intracellular copper pools demonstrated a role for *xan* cluster metabolites in the accumulation of copper. *A. fumigatus* coculture with a variety of human pathogenic fungi and bacteria established copper-dependent antimicrobial properties of *xan* BGC metabolites, including inhibition of laccase activity. Remediation of xanthocillin-treated *Pseudomonas aeruginosa* growth by copper supported the copper-chelating properties of *xan* BGC isocyanide products. The existence of the *xan* BGC in several filamentous fungi suggests a heretofore unknown role of eukaryotic natural products in copper homeostasis and mediation of interactions with competing microbes.

copper | aspergillus | chalkophore | isocyanide | fungi

Aspergillus fumigatus is a ubiquitous, filamentous fungus that exists in the environment as a saprophyte, feeding on dead organic matter. It is also the primary causative agent of invasive aspergillosis, a disease with a mortality rate of over 90% in the most severe cases (1, 2). In both environments, *A. fumigatus* is a common microbiome constituent [e.g., respiratory tract biofilms with pathogenic bacteria including *Pseudomonas aeruginosa* (3), staphylococci (4) and *Stenotrophomonas* spp (5); or soil communities composed of numerous fungi, bacteria, and protists (6, 7)]. *A. fumigatus* produces diverse secondary metabolites that play important roles in interspecific competition in these diverse environments (8).

Functions of *A. fumigatus* secondary metabolites include regulation of trace element homeostasis, assuring sufficiency for use as cofactors in enzymes while limiting their toxic effects (9, 10). For example, *A. fumigatus* produces a variety of intracellular and extracellular siderophores that coordinate acquisition and storage of iron (11, 12). Similar to iron, copper is a micronutrient required for the function of a variety of enzymes, including superoxide dismutases (SODs) (13), cytochrome *c* oxidase (14), and proteins involved in reductive iron uptake (e.g., FetC) (12). While essential, copper also participates in Fenton chemistry by reacting with hydrogen peroxide to generate toxic hydroxyl radicals (15) and can also displace other metal cofactors (e.g., Fe, Zn) in enzymes, rendering them inert (16). Thus, intracellular copper content must be precisely balanced.

Small-molecule regulators of copper homeostasis have been identified in bacteria but have yet to be described in fungi. For example, the methanobactins have been shown to be essential for copper uptake in methanotrophic bacteria, necessary for the functioning of copper-dependent methane monooxygenase (17, 18). The small molecule yersiniabactin, a nonribosomal peptide/polyketide hybrid, is a virulence factor produced by several pathogenic strains of *Escherichia coli* and acts to mitigate the toxicity of copper by binding to it, but also ensures adequate supply of copper to cells (19–21). The bacterium *Streptomyces thioluteus* produces and secretes SF2768, an isocyanide that has been demonstrated to be responsible for copper uptake (22), and the entomopathogenic bacterium *Xenorhabdus nematophila* produces the virulence factor rhabduscin, also an isocyanide, which has been shown to inhibit the insect immune defense copper-dependent laccase enzyme (23).

The first fungal isocyanide biosynthetic gene cluster (BGC) was recently identified in *A. fumigatus* (24). The *xan* BGC, including seven genes *xanA* to *xanG* (Fig. 1*A*), is regulated by the copper-binding transcription factors AceA and MacA and encodes the biosynthetic pathway for the isocyanide xanthocillin and several related compounds (24). Using chemical and genetic tools, we here demonstrate that *xan* BGC metabolite(s) are secreted and bind

Significance

Metal homeostasis is an integral part of metabolism for any organism. A vast array of natural products are already known to mediate iron homeostasis in fungi and bacteria; however, unlike their bacterial counterparts, to date, there are no known fungal small molecules that function to maintain copper homeostasis. Discovery of copper-binding xanthocillins produced by *Aspergillus fumigatus* gives insight into mechanisms other than the extensively studied copper transporters or metalloproteins for how fungi can regulate copper. This has important ecological implications, as securing scarce nutrients is central for fitness and survival. Conservation of the xanthocillin biosynthetic machinery across filamentous fungal taxa offers a new paradigm in eukaryotic metal homeostasis.

Author contributions: N.R., T.H.W., and N.P.K. designed research; N.R., T.H.W., A.S., and K.C. performed research; C.C., S.H., M.D., J.A.L.-F., and F.C.S. contributed new reagents/analytic tools; N.R., T.H.W., J.A.L.-F., F.C.S., and N.P.K. analyzed data; and N.R. and N.P.K. wrote the paper.

The authors declare no competing interest.

This article is a PNAS Direct Submission.

[1]To whom correspondence may be addressed. Email: npkeller@wisc.edu.

This article contains supporting information online at https://www.pnas.org/lookup/suppl/doi:10.1073/pnas.2015224118/-/DCSupplemental.

Published February 15, 2021.

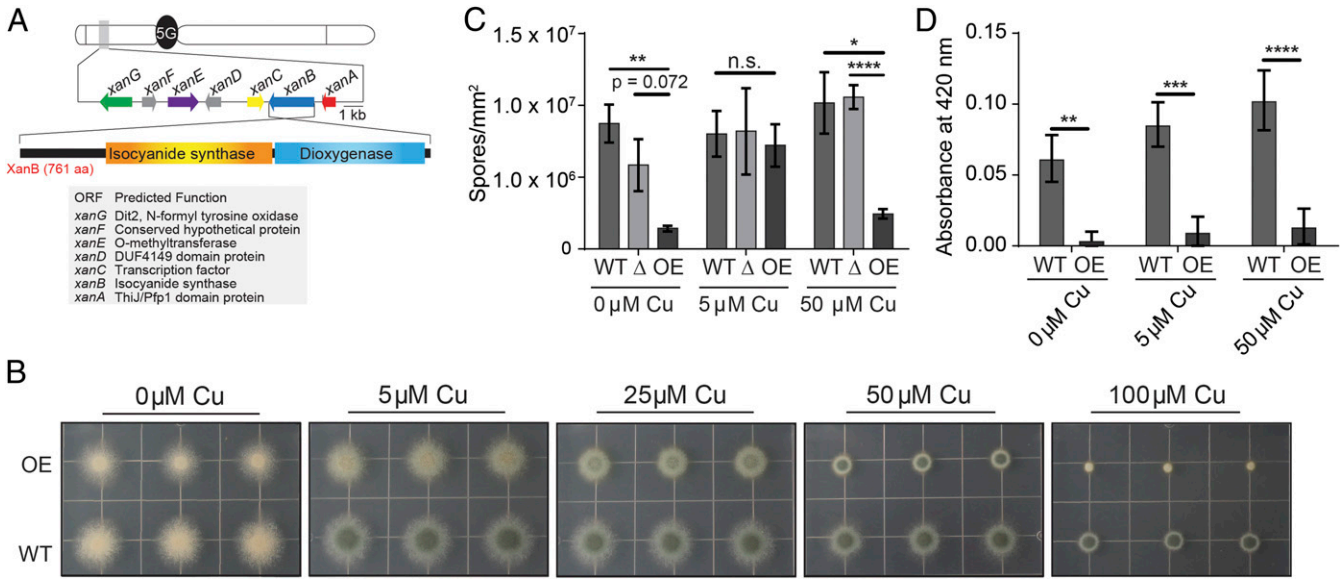

Fig. 1. The response of *xan* cluster mutants to copper stress yields a copper-dependent pigmentation phenotype. (*A*) The *xan* gene cluster responsible for the production of xanthocillin derivatives contains seven genes: *xanA* (ThiJ/Pfp1 domain protein with homology to isocyanide hydratases; red), *xanB* (two-domain isocyanide synthase-dioxygenase; blue), *xanC* (C6 transcription factor; yellow), *xanD* (DUF4149 domain protein; gray), *xanE* (O-methyltransferase; purple), *xanF* (conserved hypothetical protein; gray), and *xanG* (P450 monooxygenase homology to the yeast enzyme Dit2; green). (*B*) Growth of OE::*xanC* mutants on solid GMM supplemented with $CuSO_4$. (*C*) Sporulation of *xanC* mutants on solid GMM. (*D*) ABTS laccase activity assay of *xanC* mutants when grown on solid media supplemented with $CuSO_4$. Statistical analyses were performed using Student's *t* test, and shown is the mean with SEM of three replicates. OE, OE::*xanC*; Δ, Δ*xanC*; WT, wild type (*$P < 0.05$, **$P < 0.01$, ***$P < 0.001$, ****$P < 0.0001$).

copper, affecting cellular copper levels in *A. fumigatus* and mediating copper-dependent interactions with competing microbes. Overexpression of the *xan* BGC inhibits endogenous and exogenous laccase activity and demonstrates metal-dependent broad-spectrum antimicrobial activity. Xanthocillin recapitulates the *xan* BGC copper-dependent antibacterial activity at micromolar concentrations. This represents a characterization of copper-binding small molecules produced by a eukaryote. Conservation of the *xan* BGC in several filamentous fungi suggests a possibly widespread role for these natural products in fungal copper homeostasis and microbial competition.

Results

***xanC* Overexpression Results in Copper-Dependent Pigmentation.** Based on the finding that the *xan* BGC is regulated by copper-binding transcription factors, we investigated the effects of different levels of copper supplementation on the overexpression mutant of the transcription factor *xanC*, in which production of xanthocillin and other *xan* metabolites is constitutively increased. To achieve this, we inoculated plates of glucose minimal medium (GMM) supplemented with various amounts of copper with the *xan* cluster overexpression mutant (Fig. 1*B*). The OE::*xanC* mutant displayed a growth defect relative to the wild type control across all levels of copper and had a spore pigmentation phenotype when grown on media containing 0 μM and 5 μM $CuSO_4$ that is rescued as the copper concentration increases. However, at the highest tested concentration (100 μM $CuSO_4$), growth of the OE::*xanC* mutant was almost completely suppressed, possibly due to combined toxicity of copper and/or the *xan* BGC metabolites, whereas growth of wild type (and Δ*xanC*; shown later in Fig. 3*B*) was not as strongly affected. The pigmentation phenotype of OE::*xanC* at low copper concentrations is similar to the pigmentation defect of the wild type grown under copper limiting conditions, suggesting that overexpression of the *xan* BGC is causing a copper deficiency. To confirm that this is indeed a pigmentation defect and not a defect in sporulation, we assessed the sporulation of the *xanC* mutants and found that there was no significant difference in sporulation between the wild type and OE::*xanC* mutant at 5 μM copper (Fig. 1*C*).

We hypothesized that both the pigmentation defect and poor growth of OE::*xanC* could be partly due to decreased functionality of copper-dependent proteins (e.g., SODs and spore laccases; *SI Appendix*, Fig. S1). Indeed, assays measuring the activity of laccase, a copper-dependent enzyme, showed reduced activity in the OE::*xanC* strain relative to wild type at all levels of copper tested (Fig. 1*D*). This likely explains the spore pigmentation defect of this strain at 5 μM $CuSO_4$, as two copper-dependent laccases are required for production of DHN-melanin in *A. fumigatus* (25). Taken together, these data suggested that metabolites produced by the *xan* BGC can inhibit copper-dependent processes in *A. fumigatus*.

Gene Deletions in the *xan* BGC Confirm Their Role in the Biosynthetic Pathway. To validate our previously proposed pathway for xanthocillin biosynthesis (24) and to gain knowledge of the types of metabolites synthesized by the *xan* BGC, we created a series of double mutants by deleting each *xan* gene in the OE::*xanC* background (Fig. 2*A*). Comparative metabolomic analysis via liquid chromatography/high-resolution mass spectrometry (LC-HRMS) of OE::*xanC* with the OE::*xanC*Δ*xanB* double mutant showed that production of all *xan*-dependent compounds was abolished, consistent with the proposed function of XanB as the isocyanide synthase (Fig. 2 *B*–*H* and *SI Appendix*, Table S1). LC-HRMS analysis of the OE::*xanC*Δ*xanG* double mutant revealed accumulation of a shunt metabolite (Fig. 2*H*) derived from a monomeric isocyanide precursor for the dimeric downstream metabolites, e.g., xanthocillin, whose production was abolished. Analysis of its tandem mass spectrometry (MS) spectra and molecular formulae suggested that the monomeric shunt metabolite represented a dehydrogenated formyl tyrosine (Fig. 2*H*, *3*, and *SI Appendix*, Table S2). This result suggested that tyrosine is converted into the monomer in a two-step sequence analogous to bacterial PvcA-PvcB isocyanide synthase (26), followed

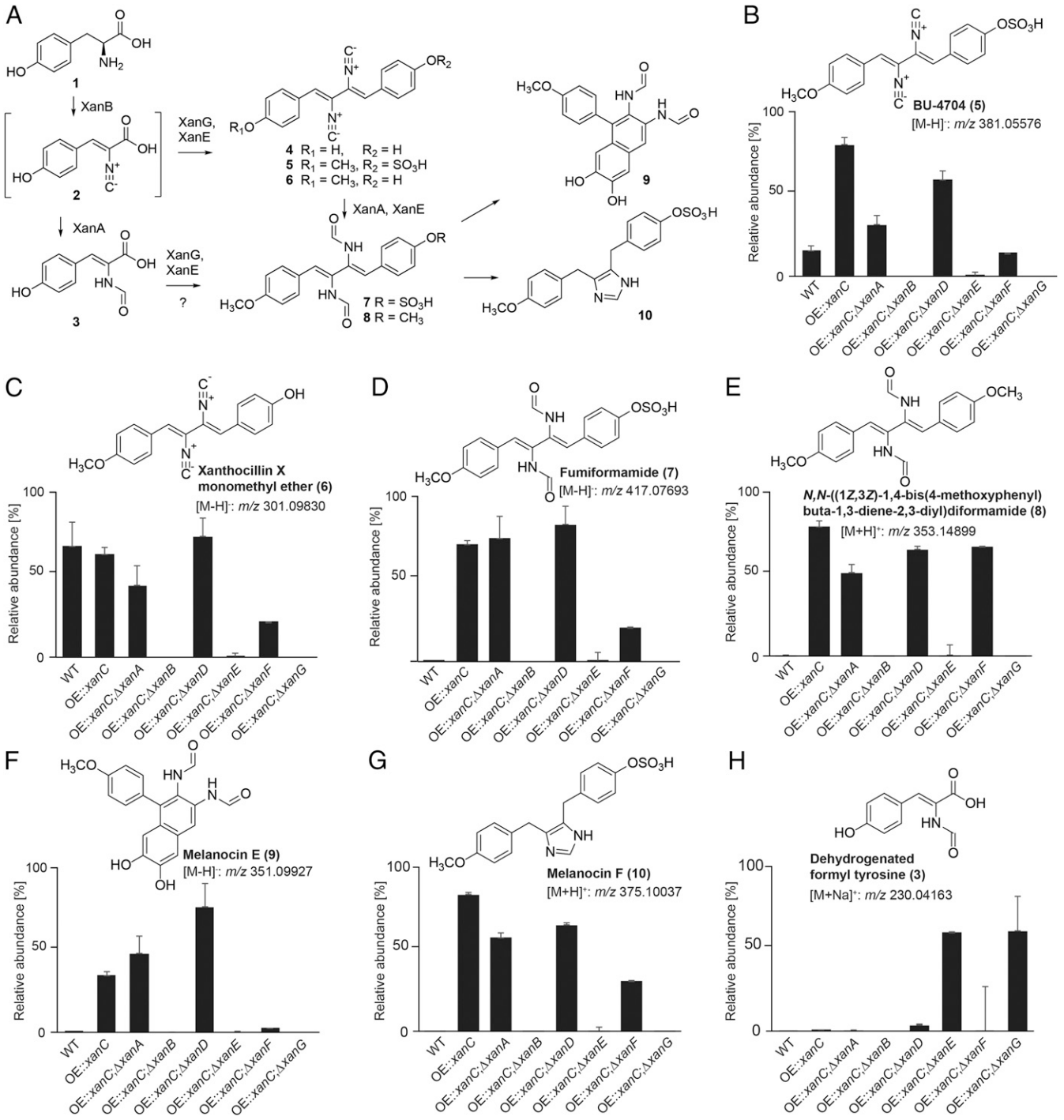

Fig. 2. *xan* gene cluster and putative functions of encoded proteins. (*A*) Putative biosynthesis of xanthocillin derivatives in *A. fumigatus*. Results from the present study further support the *xan* BGC biosynthetic pathway proposed in our previous study (24). Isocyanide containing intermediate (*2*) produced from tyrosine (*1*) by XanB is dimerized to form xanthocillin (*4*) and related isocyanides (BU-4704, *5*; and xanthocillin X monomethyl ether, *6*) by XanG. A dehydrogenated formyl tyrosine (*3*) likely represents a shunt metabolite derived from *2*. Xanthocillins are converted into the corresponding formyl derivatives [fumiformamide, *7*; and *N,N*-([1Z,3Z]-1,4-bis[4-methoxyphenyl]buta-1,3-diene-2,3-diyl)diformamide, *8*] by XanA and other isocyanide hydratases, which can undergo additional transformations to produce melanocin E (*9*) and melanocin F (*10*). Methylation of hydroxyl moieties in xanthocillin derivatives was likely introduced by XanE. (*B–H*) Relative abundances, as determined by HPLC-HRMS in ESI^+ or ESI^- mode, of xanthocillin derivatives in WT, OE::*xanC*, and a series of double mutants in which individual *xan* genes were deleted in the OE::*xanC* background. WT, wild type.

by dimerization of the monomer by XanG. Deletion of *xanE* in the OE::*xanC* background resulted in decreased total isocyanide production and especially methylated xanthocillin derivatives, in agreement with the proposed role of XanE as a methyl transferase. In contrast, comparing the metabolomes of OE::*xanC* and OE::*xanC*Δ*xanA*, we did not observe any significant changes in the abundances of the *xan*-dependent metabolites, suggesting that *xanA* is not required for the conversion of the isocyanide moiety to

its *N*-formyl derivative, even though XanA shares homology with previously studied isocyanide hydratases. Similarly, deletion of XanD, a small DUF4149 protein, did not affect levels of isocyanide derivatives to the OE::*xanC* strain, indicating that *xanD* is not involved in biosynthesis of any of the known *xan* BGC metabolites. Deletion of the hypothetical protein XanF results in decreased isocyanide production relative to wild type. BLAST analysis of XanF indicates the presence of a methyltransferase domain, suggesting that it may work with XanE to methylate the xanthocillin. However, it is also possible that, in the process of deleting XanF, the flanking genes, XanG and/or XanE, were disrupted or down-regulated during transformation. Besides xanthocillin derivatives, we detected no significant differences in accumulation of other *A. fumigatus* secondary metabolites (8) when comparing the *xanC* mutants (*SI Appendix*, Table S3). Overall, our chemical analyses showed differential accumulation of *xan* BGC products, which we then used to investigate which metabolites were responsible for the growth inhibition and copper phenotypes.

Isocyanide Accumulation Is Associated with Extracellular Copper Binding and Loss of Spore Pigmentation. Chemical profiling of the *xan* BGC mutants allowed for grouping into those that produced high levels of isocyanides (OE::*xanC*, OE::*xanC*;Δ*xanA*, and OE::*xanC*;Δ*xanD*) and those that produced much lower amounts or no *xan*-metabolites at all (OE::*xanC*;Δ*xanB*, OE::*xanC*;Δ*xanE*, OE::*xanC*;Δ*xanF*, and OE::*xanC*;Δ*xanG*; Fig. 2). Interestingly, OE::*xanC*;Δ*xanF* was the only strain that accumulated greater than wild type levels of isocyanide derivatives, but not isocyanides. Considering that some bacterial isocyanides are secreted and bind copper (18), we hypothesized that *xan* BGC-derived isocyanides would function similarly. To assess secretion, we performed a chrome azurol S (CAS) assay using the *xan* BGC mutants. The three mutants that produced the highest levels of isocyanides—OE::*xanC*, OE::*xanC*;Δ*xanA*, and OE::*xanC*;Δ*xanD*—showed similar levels of extracellular copper-chelating ability (Fig. 3*A* and *SI Appendix*, Fig. S2), whereas the other double mutants resembled more closely the copper-binding phenotype of the wild type strain. This suggested a role for *xan*-derived isocyanides as secreted copper chelators.

To further investigate whether isocyanide production was linked to copper-related phenotypes, we tested the responses to copper for each of the double mutants. We found that the OE::*xanC*;Δ*xanA* and OE::*xanC*;Δ*xanD* mutants displayed a growth and pigmentation defect compared to the OE::*xanC* strain, whereas the other mutants largely mimicked wild type growth (Fig. 3*B*). These data suggest that the *xan* BGC-derived isocyanides are the primary molecules responsible for the extracellular copper-binding phenotype and pigmentation defect.

***xan* BGC Metabolites Are Associated with Accumulation of Intracellular Copper.** In *Streptomyces thioluteus*, the chalkophore SF2768 is secreted, binds copper, and is then taken up by the bacteria (22). Based on the finding that *xan* BGC metabolites are secreted and bind copper, we asked if *xan* BGC metabolites could directly affect copper uptake. We grew the wild type, OE::*xanC*, OE::*xanC*;Δ*xanF* (representing a strain with ca. wild type levels of isocyanides but producing high amounts of several isocyanide derivatives), OE::*xanC*;Δ*xanG* (no isocyanides and no isocyanide derivatives), and Δ*xanC* (no isocyanides and no isocyanide derivatives) strains in liquid culture, either supplemented with 50 μM copper or without copper supplementation, and analyzed their intracellular copper concentrations by inductively coupled plasma (ICP) MS. We found that intracellular copper concentrations of the OE::*xanC* and OE::*xanC*;Δ*xanF* mutants were significantly elevated relative to wild type in the 50-μM copper treatment (Fig. 3*C*). There was no detectable difference in copper accumulation in the no-copper treatment. These data suggest that *xan* BGC metabolites are associated with an increase in cellular copper accumulation. Because the OE::*xanC*;Δ*xanF* mutant produced the same amount of, or fewer, isocyanides than wild type but substantial quantities of isocyanide derivatives (Fig. 2), it appears that both isocyanides and at least some derivatives are involved in copper accumulation within the fungal cell.

***xan* Mutants Inhibit Pigmentation in Fungi and Exhibit Broad-Spectrum Antimicrobial Properties.** Recent studies have shown that fungal secondary metabolites are synthesized and/or protect the producing fungus during encounters with bacteria and fungi (27); for example, the *A. fumigatus* fumicycline A BGC is induced during interactions with the soil bacterium *Streptomyces rapamycinicus* (28). Therefore, we asked whether *xan* BGC metabolites have antimicrobial properties or otherwise influence microbial interactions.

In view of the inhibitory effect of *xan* BGC metabolites on laccase activity (Fig. 1*E*), we cocultured wild type *A. fumigatus* and the OE::*xanC* mutant with *Aspergillus nidulans*. The *A. nidulans* laccase Ya is required for the green pigment of its spores, and, when Ya is inactive or deleted, the spores are yellow (29), yielding an easily scored phenotype. Fig. 4*A* shows that *A. nidulans* spores remained yellow along the border with the OE::*xanC* mutant compared to coculture with the *A. fumigatus* wild type control, where *A. nidulans* presented normal spore pigmentation. Additionally, we performed this assay using the other *xan* BGC mutants and observed that double mutants that produced isocyanides resulted in a yellow spore pigmentation along the border of the *xan* BGC mutants and *A. nidulans* (*SI Appendix*, Fig. S3*A*). We then grew the OE::*xanC* mutant alongside two other fungi that require laccase activity for either spore pigmentation in the case of *Aspergillus flavus* (30) or capsule melanization in the case of *Cryptococcus neoformans* (31) (*SI Appendix*, Fig. S3 *B* and *C*). In both cocultures, pigmentation was inhibited, as exhibited by yellow spore formation in *A. flavus* and reduction of melanization in *C. neoformans*. As with *A. nidulans*, pigmentation in both *A. flavus* and *C. neoformans* was rescued by supplementation with 50 μM $CuSO_4$.

To further investigate whether the *xan* BGC metabolites have antimicrobial properties, actively growing cultures of *A. fumigatus* mutants were cocultured with representative microbes. We observed significant inhibition of *Staphylococcus aureus*, *Candida albicans*, and *Salmonella enterica*, as well as loss of blue pigmentation in *P. aeruginosa* (PAO1) next to the OE::*xanC* mutant (Fig. 4*B* and *SI Appendix*, Fig. S4). The pigmentation and growth phenotypes were abolished when the media was supplemented with copper for all microbes tested, suggesting that *xan* BGC metabolites have copper-dependent antimicrobial properties, for example by inhibiting copper uptake or copper-dependent processes in other microbes.

We next tested the antimicrobial activity of *A. fumigatus* extracts against *S. aureus*, *S. enterica*, *P. aeruginosa* (PAO1), and *P. aeruginosa* (PAK). We consistently observed inhibition of growth of all tested microbes challenged with the OE::*xanC* extract (Fig. 4*C*). As with confrontations with actively growing fungus (Fig. 4*B* and *SI Appendix*, Fig. S4), we found that addition of copper rescued the growth defect of *P. aeruginosa* when challenged with the OE::*xanC* extract (*SI Appendix*, Fig. S5). To narrow down the *xan* BGC metabolites responsible for this activity, we performed the assay again using extracts from the double mutants. There was consistent antibacterial activity in extracts from the double mutants that produce the highest concentration of isocyanides, OE::*xanC*;Δ*xanD* and OE::*xanC*;Δ*xanA*, similar to that of the OE::*xanC* (Fig. 4*D*). These data suggested that, indeed, the isocyanides were responsible for the inhibition of pigment production and antimicrobial properties.

Pure Synthetic Xanthocillin Has Potent Antibacterial Activity. The patterns of *A. fumigatus* mutant growth (Fig. 1*B*), the copper-binding properties of mutant secretions (Fig. 3*A*), and their antimicrobial activity (Fig. 4) all support a view in which *xan* BGC-derived

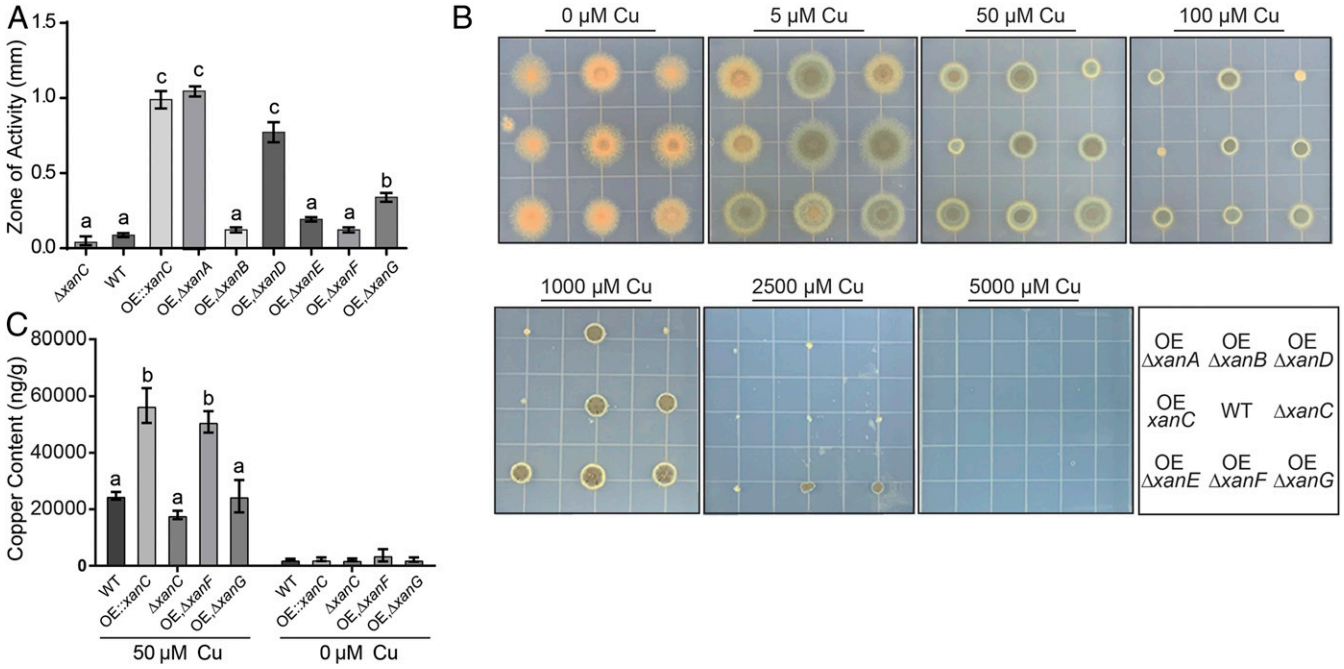

Fig. 3. Involvement of *xan* cluster metabolites in copper secretion and uptake. (*A*) Quantification of the zone of activity of CAS assay of *xan* BGC double mutants. Measurements and error bars are representative of the mean of three replicates and SE, respectively. Letters indicate statistically similar groups via an ANOVA. (*B*) Growth of the *xan* BGC double mutants on GMM supplemented with $CuSO_4$. (*Bottom Right*) Strain location key. WT, wild type; OE, Δ*xanA*, OE::*xanC*;Δ*xanA*; OE, Δ*xanB*, OE::*xanC*;Δ*xanB*; OE, Δ*xanD*, OE::*xanC*;Δ*xanD*; OE, Δ*xanE*, *OE*::*xanC*;Δ*xanE*; OE, Δ*xanF*, OE::*xanC*;Δ*xanF*; OE, Δ*xanG*, OE::*xanC*;Δ*xanG*. (*C*) Cellular copper content of *xan* cluster mutants grown in liquid shake culture lacking copper or supplemented with 50 μM $CuSO_4$ as determined by ICP-MS. Error bars represent SEM of three replicates, and statistical analysis was performed using an ANOVA. Statistical groups are designated by a letter.

isocyanides are the primary bioactive molecules from this pathway. To test this hypothesis, we compared inhibitory activities of pure xanthocillin prepared by total synthesis (32) and several *N*-formyl derivatives of the isocyanides (which no longer feature an isocyanide moiety) against *Pseudomonas* spp. We found that only xanthocillin inhibited bacterial growth (Fig. 4*E*), at a minimum inhibitory concentration (MIC) of 3.5 μM (1 μg/mL), placing it at on par with MICs of gentamicin (2 μg/mL), ceftazidime (1 μg/mL), and imipenem (1.5 μg/mL) (33). Since copper was able to abolish the inhibitory properties of the *xan* mutant extracts and when grown in coculture (Fig. 4*B* and *SI Appendix*, Fig. S5*A*), we asked if the antimicrobial activity of xanthocillin can be abolished with the addition of copper as well. We found that addition of copper at a 1:4 molar ratio relative to xanthocillin was sufficient to abolish the antimicrobial activity of the isocyanide, rescuing growth to wild type levels (Fig. 4*E*).

Metal-chelating small molecules often bind more than one metal; for instance, yersiniabactin binds to copper, nickel, and iron (19, 34), and pyoverdine, the siderophore produced by *Pseudomonas*, has been shown to bind other metals as well (35). To determine whether metals other than copper can abolish *xan* metabolite antimicrobial activity, we added different heavy metals to cultures of *P. aeruginosa* PAO1 challenged with OE::*xanC* extract. Addition of nickel, cobalt, and iron rescued the growth defect to the same extent as the copper control, whereas manganese, molybdenum, and zinc were not effective (*SI Appendix*, Fig. S5*B*). These same metals, with the exception of nickel, could also abolish the antibacterial activity of pure xanthocillin (Fig. 4*F*). These data suggest that the *xan* BGC isocyanides bind specific metal ions, including but not limited to copper.

Discussion

Copper homeostasis is a critical requirement for microbial success in all environments. Whereas tight transcriptional regulation of copper importers, exporters, and storage proteins has been well characterized in many fungi (36), including *A. fumigatus* (37), previously, no small molecule(s) had been found to contribute to copper biology in fungi. Our findings identify specific secondary metabolites, isocyanides derived from the *xan* BGC, that impact cellular copper content in fungi. Further, our work suggests that fungi synthesize copper-binding small molecules as a mechanism for copper uptake, as has been shown for a small but growing number of bacterial systems (12, 18, 34). We find *xan* BGC isocyanides also provide *A. fumigatus* with a competitive edge in coculture challenge and suggest that they may have a role as antimicrobials in the environment and could potentially be repurposed for clinical uses.

Through the creation of *xan* BGC double mutants, we provide compelling evidence that the isocyanide moieties of this cluster are required to bind copper and increase cellular copper content. Only the three mutants that accumulated the highest concentration of isocyanides (OE::*xanC*;Δ*xanA*, OE::*xanC*;Δ*xanD*, and OE::*xanC*) showed positive CAS assay results and laccase pigmentation defects, though the OE::*xanC*;Δ*xanF* exhibited a minor pigmentation defect (Figs. 1 and 3). Additionally, the OE::*xanC*;Δ*xanF* displayed similar levels of copper accumulation to the OE::*xanC*, suggesting that the isocyanide derivatives may also play a role in increasing cellular copper content.

Although our data suggest that the *xan* BGC contributes to cellular copper sufficiency, we note that the Δ*xanC* strain, which does not produce detectable amounts of *xan* BGC metabolites, retained wild type levels of intracellular copper content. It is possible that other copper uptake mechanisms, such as the copper importers CtrA2 and CtrC, can compensate for the absence of *xan* BGC metabolites. We also need to reconcile the apparent contradiction where mutants exhibit both a pigmentation defect associated with a copper deficiency and the accumulation of cellular copper. This could be due to either 1) *xan* BGC metabolite overproduction resulting in copper accumulation that is not bioavailable or 2)

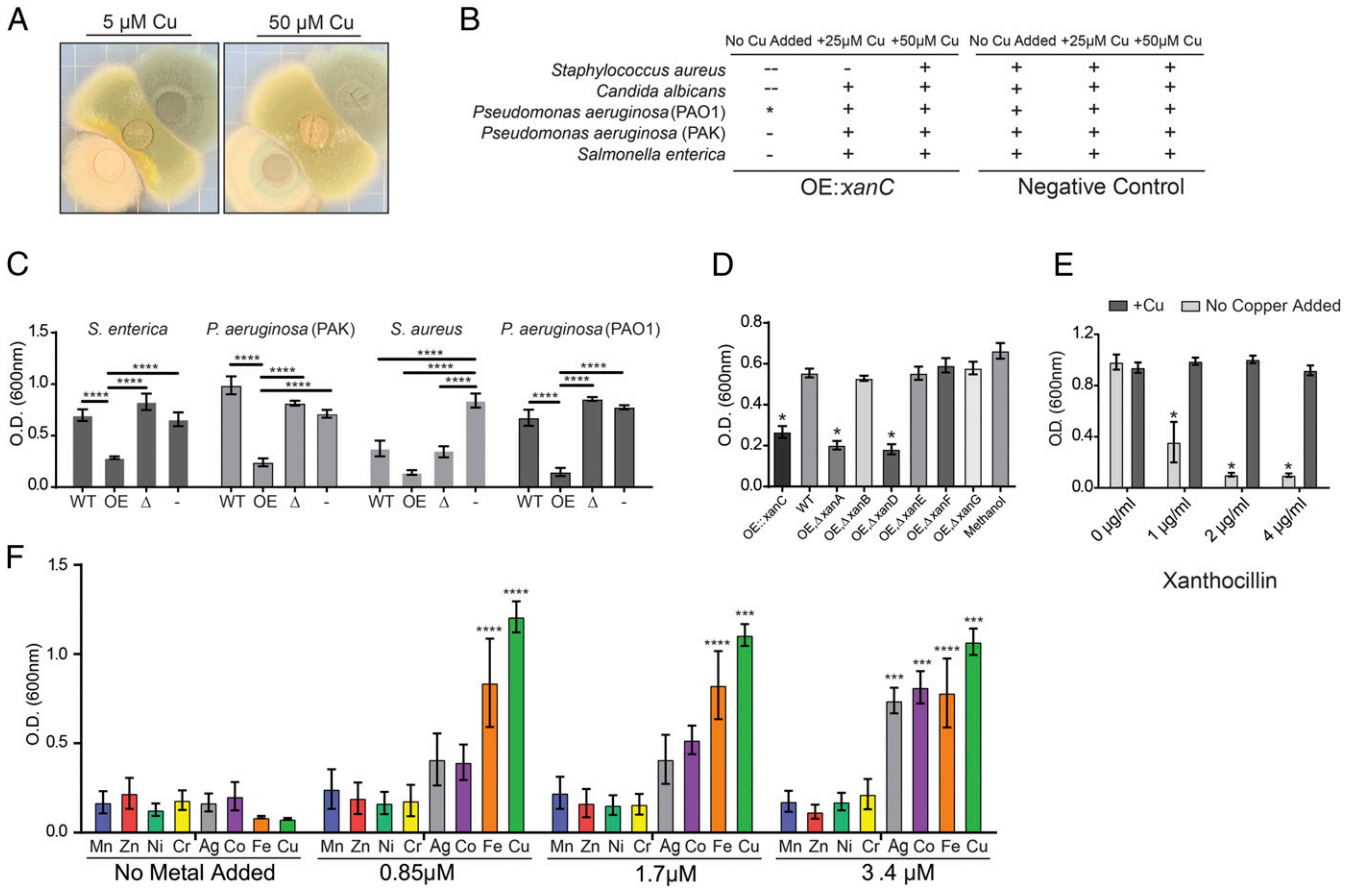

Fig. 4. *xan* cluster metabolite affects growth and copper-dependent processes of microorganisms in a metal-dependent fashion. (*A*) Coculture of *A. nidulans* (middle of plate) with wild type *A. fumigatus* (top right of plate) and the OE::*xanC* mutant (bottom left of plate) on solid GMM supplemented with $CuSO_4$. (*B*) Cocultures of *xan* mutants with microorganisms grown on solid LB. Growth inhibition of the indicate microbe was qualitatively assessed by visually inspecting the relative sizes of the zone of inhibition around the agar plugs. –, inhibition; -, partial inhibition; +, no inhibition; *, inhibits pigment production. (*C*) Growth assay of microorganisms challenged with WT, OE::*xanC*, and Δ*xanC* extracts. OE, OE::*xanC*; WT, wild type; Δ, Δ*xanC*; -, methanol (vehicle control). (*D*) Growth assay of *P. aeruginosa* (PAO1) challenged with *xan* BGC double-mutant extracts. WT, wild type; OE, Δ*xanA*, OE::*xanC*;Δ*xanA*; OE, Δ*xanB*, OE::*xanC*;Δ*xanB*; OE, Δ*xanD*, OE::*xanC*;Δ*xanD*; OE, Δ*xanE*, *OE*::*xanC*;Δ*xanE*; OE, Δ*xanF*, OE::*xanC*;Δ*xanF*; OE, Δ*xanG*, OE::*xanC*;Δ*xanG*. (*E*) *P. aeruginosa* PAO1 challenged with purified synthetic xanthocillin with and without 3.5 μM $CuSO_4$ supplemented. (*F*) *P. aeruginosa* PAO1 challenged with 1 μg/mL purified synthetic xanthocillin and supplemented with heavy metals. Statistical analyses were performed using an ANOVA comparing to WT (*D*), comparing within each xanthocillin treatment (*E*), or comparing to growth at 0 μM of the indicated metal treatment (*F*). Error bars represent SEM of experiments performed in triplicate (*$P < 0.05$, **$P < 0.01$, ***$P < 0.001$, ****$P < 0.0001$).

overproduction of *xan* BGC metabolites resulting in a copper-limited microenvironment, preventing copper from being accessible to extracellular laccases. The former would explain the growth defect of the OE::*xanC* strain when grown using the low-copper condition by exacerbating the copper deficiency and using the high-copper condition where copper is potentially hyperaccumulated to toxic levels. However, whereas the role of *xan* BGC-derived metabolites for copper sufficiency will require further study, our data demonstrate that *xan* BGC metabolites are secreted, bind copper, and inhibit activity of copper-requiring enzymes.

Our results comparing different *xan* BGC mutants and purified *xan* BGC metabolites strongly suggest that the isocyanide moieties of the *xan* BGC metabolites were responsible for their antimicrobial activities. The isocyanide-producing mutants that showed high CAS activity, greatest pigmentation defects, and growth defects also inhibited or altered bacterial growth most strongly. Isocyanides also inhibited pigmentation in *P. aeruginosa* (PAO1), which we hypothesize is due to an interference with the copper–pyocyanin complex (38). Furthermore, xanthocillin but not *N*-formyl derivatives lacking the isocyanide moiety significantly inhibited *Pseudomonas* growth (Fig. 4 *E* and *F* and *SI Appendix*, Fig. S6). Antimicrobial or laccase-inhibiting properties were abolished by increasing copper concentrations in media (Fig. 4). Additional heavy metals such as silver, cobalt, and iron were able to rescue the growth defect of the bacteria challenged with xanthocillin, suggesting that the isocyanides bind to a subset of metal cations, with xanthocillin itself having the highest affinity for copper under the tested conditions. Overall, this indicates that isocyanides could be used by *A. fumigatus* to compete with other microbes by either depriving competitors of essential, scarce nutrients or by directly inhibiting metal-dependent processes. This supposition is strongly supported by a previous study where coculture of the bacterium *Streptomyces peucetius* with *A. fumigatus* induced synthesis of several *xan* BGC metabolites associated with bacterial inhibition [at the time, the *xan* cluster had not been identified (39)].

Although we were unable to obtain this *Streptomyces* isolate to confirm *xan* BGC induction, we did find that *xanB* encoding the xanthocillin isocyanide synthase is induced by hydrogen peroxide (*SI Appendix*, Fig. S7*A*), suggesting a possible role for this metabolite in various stress responses. This response may tie in with copper Fenton chemistry, as chelation of copper would be expected to reduce the damage wrought by Fenton chemistry. In addition,

we note that the entire BGC is differentially regulated by mutants in the hexadehydroastechrome biosynthesis (40). Considering that hexadehydroastechrome binds iron (41), this may suggest copper/iron cross-talk can be in part mediated via natural product synthesis in fungi, a further study of this lab.

Our results clarify the roles of most Xan proteins in the biosynthesis of the *xan* BGC metabolites, solidifying the proposed biosynthetic pathway presented in a previous study (24). Two *xan* proteins that did not affect biosynthesis under the tested conditions were XanD and XanA. XanD is a protein of unknown function; however, XanA shares homology with previously studied isocyanide hydratases (42). In bacteria, isocyanide (isonitrile) hydratases convert isocyanides to their less toxic *N*-substituted formamides (43). Hence, we speculated that the OE::*xanCΔxanA* strain would be sicker than OE::*xanC* by virtue of producing more isocyanides and less *N*-formyl derivatives. This was not the case. One possible explanation for the apparent lack of involvement of XanA in this pathway is that there are six other putative isocyanide hydratases in the *A. fumigatus* genome. This redundancy suggests that at least one of these other proteins is able to convert the *xan* isocyanides to their *N*-formyl derivative, thus compensating for the absence of XanA.

In conclusion, here we report small molecule(s) produced by a fungus that specifically mediate copper-dependent processes. This work adds a eukaryotic system to the many reported bacterial species known to use small molecules to bind copper, possibly functioning in copper uptake, and in related interactions with other organisms. Although this work focused on *A. fumigatus*, it seems likely that similar molecules play analogous roles in other fungi, as the *xan* BGC is conserved in several fungal species (24). As with *A. fumigatus*, many of these fungi possess more than one isocyanide synthase-containing BGC. The characterization of these additional BGCs should provide exciting new insights in the functions of isocyanides in the microbial world.

Materials and Methods

Mutant Construction. Double-joint PCR used to generate DNA constructs for transformation of all fungal stains was carried out as described previously (44). All strains and primers used in this study are listed in the supplemental materials (*SI Appendix*, Tables S4 and S5). Further details of the strain construction are provided in the *SI Appendix*.

Fungal Growth Conditions and Physiological Assays. *Aspergillus* strains were grown on GMM and manipulated as described previously (45, 46). For liquid shake cultures, 50 mL of GMM was inoculated with 1×10^6 spores per milliliter and incubated at 37 °C, shaking at 250 rpm for 48 h. Lyophilized mycelia were obtained by filtering cultures through MiraCloth, freezing in liquid nitrogen, and lyophilizing overnight. For sporulation assay, strains were suspended in 10 mL molten GMM and overlayed onto a plate of GMM. An agar plug was transferred to a solution of 0.01% Tween and homogenized. Samples were then diluted and spores enumerated using a hemocytometer.

RNA Extraction and qRT-PCR. Total culture mycelia from a liquid shake culture was filtered, flash-frozen in liquid nitrogen, and lyophilized. RNA was extracted using the QIAzol Lysis Reagent (Qiagen). RNA was then subjected to a DNase I digestion (New England Biolabs) and reverse-transcribed using iScript cDNA synthesis kit (Bio-Rad). Semiquantitative PCR was performed by amplifying the gene of interest via designed primers (*SI Appendix*, Table S5) and using *A. fumigatus* actin as a loading control.

CAS Assay. CAS assay plates were prepared as described previously (47). A sterile razor was used to remove half of the CAS media, and 10 mL of warm molten GMM was then inoculated with 1×10^7 spores and poured into the vacant space. The plates were then allowed to solidify and incubated for 5 d at 37 °C in the dark. The zone of activity was quantified by measuring the distance between the growing mycelia and the edge of the Cu–CAS complex with a ruler.

Laccase Activity Assay. Plates were incubated with 1×10^7 spores, incubated for 48 h at 37 °C, and then flushed with 10 mL of 1 mM 2,2′-azino-bis(3-ethylbenzothiazoline)-6-sulphonic acid (ABTS). They were then incubated at ambient temperature for an additional 24 h. Aliquots of supernatant (200 μL) were transferred to a 96-well plate, and absorbance was measured at 420 nm. Data were quantified and normalized to the negative control, uninoculated plates flushed with 1 mM ABTS.

Metabolite Extraction. Overlay cultures were frozen using liquid nitrogen and lyophilized. The lyophilized samples were extracted with 20 mL of ethyl acetate-methanol (9:1) for 1.5 h with vigorous stirring. Extracts were filtered over cotton, evaporated to dryness, and stored in 4-mL vials. Crude extracts were suspended in 0.5 mL of methanol and centrifuged to remove insoluble materials, and the supernatant was analyzed by ultra–high-performance liquid chromatography high-resolution mass spectrometry (UHPLC-HRMS).

High-Resolution High-Performance LC-MS Analytical Methods and Equipment Overview. High-resolution high-performance LC-MS (HPLC-HRMS) was performed on a Thermo Scientific-Dionex Ultimate 3000 UHPLC system equipped with a diode array detector and connected to a Thermo Scientific Q Exactive Orbitrap mass spectrometer operated in electrospray-positive (ESI^+) or electrospray-negative (ESI^-) ionization mode. An Agilent Zorbax RRHD Eclipse XDB-C18 column (2.1 × 100 mm, 1.8-μm particle diameter) was used with acetonitrile (organic phase) and 0.1% formic acid in water (aqueous phase) as solvents at a flow rate of 0.5 mL/min. A solvent gradient scheme was used, starting at 2% organic for 1 min, followed by a linear increase to 100% organic over 14 min, holding at 100% organic for 2.5 min, decreasing back to 2% organic for 0.1 min, and holding at 2% organic for the final 1.4 min, for a total of 18 min.

ICP-MS. Mycelia were analyzed by ICP-MS after acid digestion. One hundred microliters of concentrated trace metal-grade nitric acid, 50 μL of 18 MΩ water, and 25 μL of 500 ng/mL scandium used as internal standard solution were added to the samples in a metal-free 5-mL conical vial. After the digestion was carried out in a heating block at 90 °C for 2 h with venting every 20 min, the samples were brought to 2.5 mL with 18 MΩ water. The samples were then analyzed for total Cu content in an Agilent 7500 ICP-MS system with a Cetac ASX-520 autosampler contained in an acrylic box. The ICP-MS system was configured with a Micromist nebulizer, a double-pass Scott spray chamber held at 2 °C, a 2.5-mm torch with platinum shield torch, and nickel sample and skimmer cones. The instrument was run with 3.5 mL/min of helium in energy discrimination mode. The external calibration method was used with a calibration range of 0.05 to 25 ng/mL The mass of the samples (200 to 800 μg) needed for the quantification of Cu was calculated by measuring the phosphorous content in the digested samples according to a previous work (48).

Total Synthesis of Xanthocillin. Synthetic xanthocillin was prepared in 10 steps from commercially available 4-hydroxybenzaldehyde by following the approach developed by Yamaguchi et al. (32). The NMR and HRMS data of the synthetic sample (*SI Appendix*, Fig. S7) match with the reported ones. Further details of xanthocillin synthesis are provided in the *SI Appendix*.

Cocultures and Growth Conditions. Microbes for coculture experiments were activated from glycerol stock onto plates of lysogeny broth (LB) or yeast peptone dextrose (YPD), streaking for single colonies. A single colony was then selected and inoculated into 5 mL of liquid LB or YPD, shaking at 37 °C or 30 °C (*C. albicans*) overnight. Coculture experiments were performed by transferring GMM agar plugs of an actively growing overlay fungal culture to solid LB or YPD. An overlay of the bacteria/fungi was generated by suspending microorganisms to a final OD_{600} of 0.05 in 10 mL of molten top agar and dispensing onto the LB containing the agar plugs. The plates were then incubated overnight at either 37 °C or 30 °C (*C. albicans*). Zones of inhibition were visually evaluated to determine inhibition of growth. For cocultures involving *A. nidulans* or *A. flavus*, GMM containing various levels of copper was inoculated with 1×10^7 spores of *Aspergillus* spp. and preincubated for 24 h at 37 °C. The plates were then inoculated with 1×10^7 spores of the *xan* mutant strains and incubated for an additional 72 h at 37 °C. For 96-well plate assays, overnight cultures were diluted to an OD_{600} of 0.05 in liquid LB, and 190 μL was dispensed into a well containing 10 μL of the corresponding extract/xanthocillin. For coculture assays involving *C. neoformans*, overnight cultures were grown in YPD overnight at 30 °C. The culture was then streaked on a plate of YPD containing 1 mM L-DOPA and allowed to incubate for 24 h at 30 °C. Agar plugs of actively growing fungal culture were then transferred and allowed to incubate for an additional 24 h before visual inhibition of laccases was assessed.

Data Availability. All study data are included in the article and/or supporting information.

ACKNOWLEDGMENTS. Partial funding for this work was provided by the NIH under Grants R01GM112739 to F.C.S. and N.P.K., R35GM128570 to M.D., and T32GM008349 to N.R. The funders had no role in study design, data collection and interpretation, or the decision to submit the work for publication.

1. J. A. Sugui, K. J. Kwon-Chung, P. R. Juvvadi, J.-P. Latgé, W. J. Steinbach, Aspergillus fumigatus and related species. *Cold Spring Harb. Perspect. Med.* **5**, a019786 (2014).
2. F. S. Taccone *et al*.; AspICU Study Investigators, Epidemiology of invasive aspergillosis in critically ill patients: Clinical presentation, underlying conditions, and outcomes. *Crit. Care* **19**, 7 (2015).
3. J. Scott *et al*., *Pseudomonas aeruginosa*-derived volatile sulfur compounds promote distal *Aspergillus fumigatus* growth and a synergistic pathogen-pathogen interaction that increases pathogenicity in Co-infection. *Front. Microbiol.* **10**, 2311 (2019).
4. S. Junge *et al*., Factors associated with worse lung function in cystic fibrosis patients with persistent staphylococcus aureus. *PLoS One* **11**, e0166220 (2016).
5. E. Melloul *et al*., Characteristics of aspergillus fumigatus in association with stenotrophomonas maltophilia in an in vitro model of mixed biofilm. *PLoS One* **11**, e0166325 (2016).
6. A. Antoniou, M. D. Tsolakidou, I. A. Stringlis, I. S. Pantelides, Rhizosphere microbiome recruited from a suppressive compost improves plant fitness and increases protection against vascular wilt pathogens of tomato. *Front Plant Sci* **8**, 2022 (2017).
7. F. A. Muotoe-Okafor, H. C. Gugnani, In vitro interactions between Histoplasma capsulatum var. duboisii and other fungi. *Mycoses* **40**, 309–312 (1997).
8. N. Raffa, N. P. Keller, A call to arms: Mustering secondary metabolites for success and survival of an opportunistic pathogen. *PLoS Pathog.* **15**, e1007606 (2019).
9. A. Crawford, D. Wilson, Essential metals at the host-pathogen interface: Nutritional immunity and micronutrient assimilation by human fungal pathogens. *FEMS Yeast Res.* **15**, 1–11 (2015).
10. F. Gerwien, V. Skrahina, L. Kasper, B. Hube, S. Brunke, Metals in fungal virulence. *FEMS Microbiol. Rev.* **42**, 1–21 (2018).
11. M. Schrettl *et al*., Distinct roles for intra- and extracellular siderophores during Aspergillus fumigatus infection. *PLoS Pathog.* **3**, 1195–1207 (2007).
12. M. Schrettl *et al*., Siderophore biosynthesis but not reductive iron assimilation is essential for *Aspergillus fumigatus* virulence. *J. Exp. Med.* **200**, 1213–1219 (2004).
13. K. Lambou, C. Lamarre, R. Beau, N. Dufour, J. P. Latge, Functional analysis of the superoxide dismutase family in Aspergillus fumigatus. *Mol. Microbiol.* **75**, 910–923 (2010).
14. N. Grahl, K. M. Shepardson, D. Chung, R. A. Cramer, Hypoxia and fungal pathogenesis: To air or not to air? *Eukaryot. Cell* **11**, 560–570 (2012).
15. K. Jomova *et al*., Protective role of quercetin against copper(II)-induced oxidative stress: A spectroscopic, theoretical and DNA damage study. *Food Chem. Toxicol.* **110**, 340–350 (2017).
16. A. Barwinska-Sendra, K. J. Waldron, *The Role of Intermetal Competition and Mis-Metalation in Metal Toxicity* (Elsevier Ltd., ed. 1, 2017).
17. L. M. K. Dassama, G. E. Kenney, S. Y. Ro, E. L. Zielazinski, A. C. Rosenzweig, Methanobactin transport machinery. *Proc. Natl. Acad. Sci. U.S.A.* **113**, 13027–13032 (2016).
18. G. E. Kenney, A. C. Rosenzweig, Chalkophores. *Annu. Rev. Biochem.* **87**, 645–676 (2018).
19. A. E. Robinson, J. E. Lowe, E. I. Koh, J. P. Henderson, Uropathogenic enterobacteria use the yersiniabactin metallophore system to acquire nickel. *J. Biol. Chem.* **293**, 14953–14961 (2018).
20. E. I. Koh, A. E. Robinson, N. Bandara, B. E. Rogers, J. P. Henderson, Copper import in Escherichia coli by the yersiniabactin metallophore system. *Nat. Chem. Biol.* **13**, 1016–1021 (2017).
21. K. S. Chaturvedi *et al*., Cupric yersiniabactin is a virulence-associated superoxide dismutase mimic. *ACS Chem. Biol.* **9**, 551–561 (2014).
22. L. Wang *et al*., Diisonitrile natural product SF2768 functions as a chalkophore that mediates copper acquisition in Streptomyces thioluteus. *ACS Chem. Biol.* **12**, 3067–3075 (2017).
23. J. M. Crawford, C. Portmann, X. Zhang, M. B. J. Roeffaers, J. Clardy, Small molecule perimeter defense in entomopathogenic bacteria. *Proc. Natl. Acad. Sci. U.S.A.* **109**, 10821–10826 (2012).
24. F. Y. Lim *et al*., Fungal isocyanide synthases and xanthocillin biosynthesis in Aspergillus fumigatus. *MBio* **9**, e00785-18 (2018).
25. H. F. Tsai, M. H. Wheeler, Y. C. Chang, K. J. Kwon-Chung, A developmentally regulated gene cluster involved in conidial pigment biosynthesis in Aspergillus fumigatus. *J. Bacteriol.* **181**, 6469–6477 (1999).
26. M. F. Clarke-pearson, S. F. Brady, Paerucumarin, a new metabolite produced by the pvc gene cluster from Pseudomonas aeruginosa. *J. Bacteriol.* **190**, 6927–6930 (2008).
27. N. P. Keller, Fungal secondary metabolism: Regulation, function and drug discovery. *Nat. Rev. Microbiol.* **17**, 167–180 (2019).
28. C. C. König *et al*., Bacterium induces cryptic meroterpenoid pathway in the pathogenic fungus Aspergillus fumigatus. *ChemBioChem* **14**, 938–942 (2013).
29. E. B. O'Hara, W. E. Timberlake, Molecular characterization of the Aspergillus nidulans yA locus. *Genetics* **121**, 249–254 (1989).
30. P. K. Chang *et al*., Identification of a copper-transporting ATPase involved in biosynthesis of A. flavus conidial pigment. *Appl. Microbiol. Biotechnol.* **103**, 4889–4897 (2019).
31. H. C. Eisenman *et al*., Cryptococcus neoformans laccase catalyses melanin synthesis from both D- and L-DOPA. *Microbiology (Reading)* **153**, 3954–3962 (2007).
32. T. Yamaguchi, Y. Miyake, A. Miyamura, N. Ishiwata, K. Tatsuta, Structure-activity relationships of xanthocillin derivatives as thrombopoietin receptor agonist. *J. Antibiot. (Tokyo)* **59**, 729–734 (2006).
33. J. J. Varga *et al*., Genotypic and phenotypic analyses of a Pseudomonas aeruginosa chronic bronchiectasis isolate reveal differences from cystic fibrosis and laboratory strains. *BMC Genomics* **16**, 883 (2015).
34. E. M. Nolan, A noncanonical role for Yersiniabactin in bacterial copper acquisition. *Biochemistry* **56**, 6073–6074 (2017).
35. A. Braud, F. Hoegy, K. Jezequel, T. Lebeau, I. J. Schalk, New insights into the metal specificity of the Pseudomonas aeruginosa pyoverdine-iron uptake pathway. *Environ. Microbiol.* **11**, 1079–1091 (2009).
36. C. Li, Y. Li, C. Ding, The role of copper homeostasis at the host-pathogen axis: From bacteria to fungi. *Int. J. Mol. Sci.* **20**, 1–15 (2019).
37. N. Raffa, N. Osherov, N. P. Keller, Copper utilization, regulation, and acquisition by aspergillus fumigatus. *Int. J. Mol. Sci.* **20**, 1980 (2019).
38. W. S. Moos, J. W. Rowen, Identification of a copper complex-forming fraction of pyocyanine. *Arch. Biochem. Biophys.* **43**, 88–96 (1953).
39. K. M. Zuck, S. Shipley, D. J. Newman, Induced production of N-formyl alkaloids from Aspergillus fumigatus by co-culture with Streptomyces peucetius. *J. Nat. Prod.* **74**, 1653–1657 (2011).
40. P. Wiemann *et al*., Perturbations in small molecule synthesis uncovers an iron-responsive secondary metabolite network in Aspergillus fumigatus. *Front. Microbiol.* **5**, 530 (2014).
41. W. B. Yin *et al*., A nonribosomal peptide synthetase-derived iron(III) complex from the pathogenic fungus Aspergillus fumigatus. *J. Am. Chem. Soc.* **135**, 2064–2067 (2013).
42. M. Goda, Y. Hashimoto, S. Shimizu, M. Kobayashi, Discovery of a novel enzyme, isonitrile hydratase, involved in nitrogen-carbon triple bond cleavage. *J. Biol. Chem.* **276**, 23480–23485 (2001).
43. M. Zhu *et al*., Tandem hydration of diisonitriles triggered by isonitrile hydratase in *Streptomyces thioluteus*. *Org. Lett.* **20**, 3562–3565 (2018).
44. E. Szewczyk, *et al*., Fusion PCR and gene targeting in Aspergillus nidulans. *Nat. Protoc.* **1**, 3111–3120 (2007).
45. K. Shimizu, N. P. Keller, Genetic involvement of a cAMP-dependent protein kinase in a G protein signaling pathway regulating morphological and chemical transitions in Aspergillus nidulans. *Genetics* **157**, 591–600 (2001).
46. P. Wiemann *et al*., Aspergillus fumigatus copper export machinery and reactive oxygen intermediate defense counter host copper-mediated oxidative antimicrobial offense. *Cell Rep.* **19**, 1008–1021 (2017).
47. S. Yoon, S. M. Kraemer, A. A. Dispirito, J. D. Semrau, An assay for screening microbial cultures for chalkophore production. *Environ. Microbiol. Rep.* **2**, 295–303 (2010).
48. J. A. L. Figueroa, C. A. Stiner, T. L. Radzyukevich, J. A. Heiny, Metal ion transport quantified by ICP-MS in intact cells. *Sci. Rep.* **6**, 20551 (2016).